

CrystEngComm

Accepted Manuscript



This is an *Accepted Manuscript*, which has been through the Royal Society of Chemistry peer review process and has been accepted for publication.

Accepted Manuscripts are published online shortly after acceptance, before technical editing, formatting and proof reading. Using this free service, authors can make their results available to the community, in citable form, before we publish the edited article. We will replace this *Accepted Manuscript* with the edited and formatted *Advance Article* as soon as it is available.

You can find more information about *Accepted Manuscripts* in the [Information for Authors](#).

Please note that technical editing may introduce minor changes to the text and/or graphics, which may alter content. The journal's standard [Terms & Conditions](#) and the [Ethical guidelines](#) still apply. In no event shall the Royal Society of Chemistry be held responsible for any errors or omissions in this *Accepted Manuscript* or any consequences arising from the use of any information it contains.



A Unique “Cage-in-Cage” Metal-Organic Framework based on Nested Cages from Interpenetrated Networks

Received 00th January 20xx,
Accepted 00th January 20xx

Ting-Ting Zhou[†], Zhi-Hong Xuan[†], Da-Shuai Zhang, Ze Chang*, Ying-Hui Zhang*, and Xian-He Bu

DOI: 10.1039/x0xx00000x

www.rsc.org/

A novel “cage-in-cage” metal-organic framework based on nested cages originate from two-fold interpenetrated networks was reported, which indicates the potential of interpenetration in structure modulation of cage-based MOFs.

As one class of emerging materials with versatile structures and intriguing properties, porous metal-organic frameworks (MOFs) exhibit potential applications in many fields such as gas storage and separation, catalysis, drug delivery, and chemical sensing.¹ The novelty of these materials lies in their highly ordered framework structure with well-defined internal space, which could be tailored through the modulation of organic linkers and metal centers.² Of all architectures reported, cage-based frameworks are of particularly attractive since their relatively confined pore structure could benefit the interactions between the most framework and guest molecules trapped in. Many MOFs based on different kinds of polyhedron cages have been reported in literatures up to date, including tetrahedron,³ hexahedron,⁴ octahedron⁵ and cubooctahedron,⁶ etc. Very recently, one kind of MOFs based on nested cages structures, i.e. the “cage-in-cage” structures, has been reported.^{7,8} Compared with the ordinary cage based MOFs, the successful assembly of nested cage structures are rather more complicated and many factors are required, e.g. the dimension and configuration of the ligands, the coordination geometry of the metal ions/clusters, and the consideration of charge balance, et al. Therefore the reported nested cages based MOFs are quite rare.

On the other hand, the entanglement of frameworks in porous MOFs, including interpenetration and interweaving, has been considered as a notable phenomenon with dual character. Though the reduction of accessible pore volume from the entanglement of frameworks could be a drawback for storage applications, however, it could also be an advantage since it provides opportunity for the

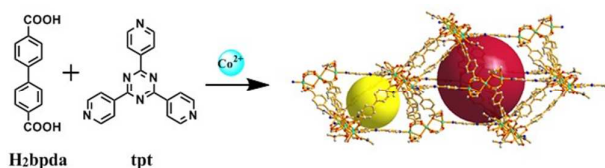


Chart. 1 The construction of MOF 1.

stabilization of open frameworks as well as the realization of structure flexibility from the displacement of networks, which is desired for separation and sensing applications.⁹ It is worth to be noticed that though the construction and tuning of interpenetration has been widely reported in MOFs¹⁰, samples based on polyhedron cages are quite rare, which could be attributed to the steric hindrance of polyhedron as building units that prevent the occurrence of interpenetration.¹¹

As a continuation of our previous work on nested “cage-in-cage” MOFs,⁸ we have been trying to investigate potential systems for the assembly of nested cage structures. During our investigation, it was found that the interpenetration of networks could be an effective method for the access of “cage-in-cage” MOFs: nested cages could be obtained through the interpenetration of MOFs networks based on polyhedron cages with matched shapes and dimensions. Herein, we report a unique MOF, $\text{Co}_3(\text{bpda}^{2-})_3(\text{tpt})_{2/3}(\text{DMF})_2$ (**1**) (H_2bpda = biphenyl-4,4'-dicarboxylic acid, tpt = 2,4,6-tris(4-pyridyl)-1,3,5-triazine, and DMF = N,N-dimethylformamide). In this MOF, the assembly of the ligands and trinuclear Co(II) clusters result in two-fold interpenetrated framework of individual network based on two kinds of cages (Chart. 1). The smaller octahedral cages from one network are perfectly nested in the larger cuboctahedral ones from the other, which reveal a novel “cage-in-cage” framework structure. Furthermore, the adsorption property of this MOF was also investigated.

MOF **1** was synthesized under solvothermal condition, and high crystalline product is readily obtained (for details, see ESI[†]). Single crystal diffraction analysis reveals that MOF **1** crystallizes in the trigonal $R\bar{3}c$ space group. The asymmetric unit of **1** contains two crystallographically independent Co(II) cations, one tpt ligand, three bpda^{2-} ligands and one DMF molecule. Every Co1 cation centres in an octahedron completed by six carboxylic oxygen atoms from six

^a Department of Chemistry, Tianjin Key Lab on Metal and Molecule-based Material Chemistry, Collaborative Innovation Center of Chemical Science and Engineering (Tianjin), Nankai University, Tianjin 300071, China. E-mail: changze@nankai.edu.cn; zhangyhi@nankai.edu.cn; FAX: 86 22 23502458

[†] These authors contribute equally to this work.

Electronic Supplementary Information (ESI) available: Crystallographic data in CIF format, experiment details, crystallographic refinement data, additional structure figures, PXRD, TGA, and adsorption enthalpy data. See DOI: 10.1039/x0xx00000x

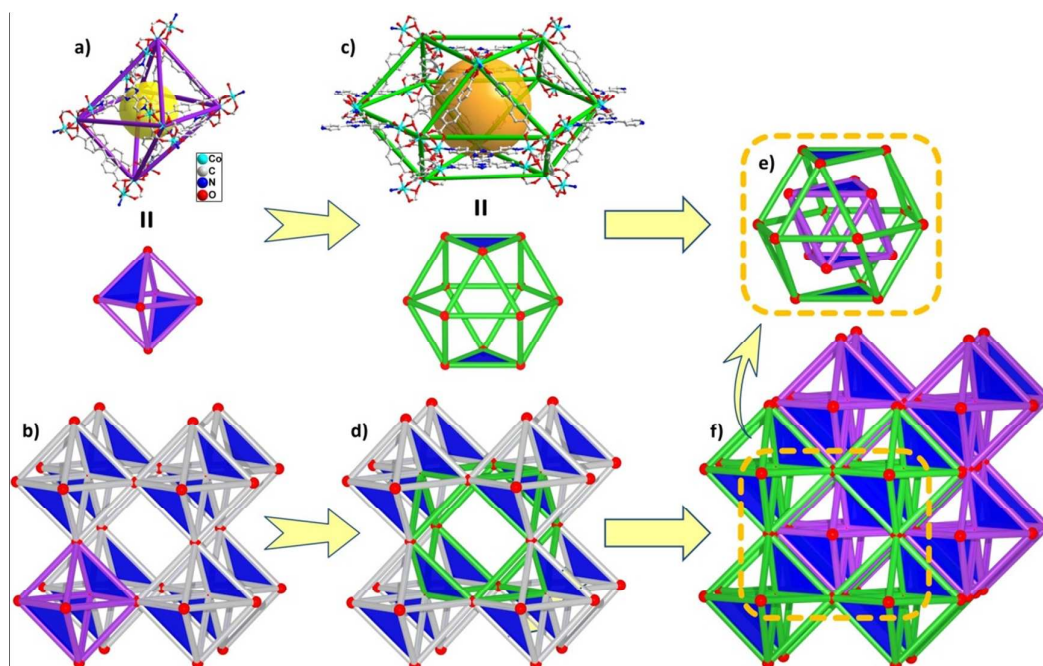


Fig. 1 a) The structure of the octahedral cage. b) The packing of octahedral cages in the individual network. c) The structure of the cuboctahedral cage. d) The formation of cuboctahedral cage in the individual network. e) The nested cages resulted from the two-fold interpenetrated networks. f) The view of interpenetrated framework. The red spheres represent for the Co clusters, the purple/green sticks represent for the linkages between the clusters depending on distinct networks, and the blue triangles represent for the tpt ligands occupied cage surfaces.

different bpda^{2-} ligands, while each Co_2 cation centres in a distorted octahedron surrounded by four carboxylate oxygen atoms from four bpda^{2-} ligand, one oxygen atom from a coordinated DMF molecule and one N atom from the pyridine group of a tpt ligand (Fig. S1a). All Co–O and Co–N distances (Co–O: 2.021(4)–2.178(4) Å; Co–N: 1.975(3)–2.062(10) Å) agree well with that reported in the literatures.^{8,12} Co_1 ion is bridged with two neighbouring Co_2 atoms by three carboxylate groups to form a linear trinuclear Co_3 cluster ($\text{Co}_2\text{--Co}_1\text{--Co}_2$ angle: $170.492(27)^\circ$). For the bpda^{2-} ligand, two kinds of linking modes were observed for: for the one, two carboxylate groups of one bpda^{2-} ligand coordinate toward Co ions in $\mu_2\text{--O;O'}$ and $\mu_2\text{--O;O';O'}$ mode, respectively (Fig. S1b); for the other, similar $\mu_2\text{--O;O'}$ mode was observed for the two carboxylate groups from one bpda^{2-} ligand (Fig. S1c). On the other hand, tpt ligand acts as tridentate ligand to link three Co_3 cluster (Fig. S1d). Each Co_3 cluster is linked to six neighbouring clusters through six bpda^{2-} and two tpt ligands, to generate a complicated three dimensional (3D) two-fold interpenetrated framework structure. The porosity of the framework is calculated to be 39.5% by PLATON.¹³ Topological simplification of the framework with TOPOS¹⁴ results in two-fold interpenetrated (3,6)-connected **loh1** topology with the vertex symbol $(4^3)_2(4^6.6^8.8^3)_3$, by treating the Co clusters and tpt ligands as 6 and 3 connected nodes, respectively. It should be noted that this is the second interpenetrated **loh1** topology network obtained in MOFs.¹⁵

Detailed inspection of **1** further unveils co-existence of two kinds of cages with distinct shapes and dimensions in the framework. As shown in Fig. 1a, six Co clusters linked by two tpt and nine bpda^{2-} ligands defined a small cage with distorted octahedral shape. In this

cage, the Co clusters serve as vertexes, and the tpt and bpda^{2-} ligands serve as edges. Two of the eight triangular faces of the cage are occupied by the tpt ligands, while the other ones left open. The diameter of the largest sphere within the cage is about 9 Å, excluding the van der Waals radius of atoms on the walls. Then the individual network in MOF **1** could be regarded as the packing of octahedral cages by sharing the Co cluster vertexes (Fig. 1b). On the other hand, the packing of eight octahedral cages result in a larger cage with novel distorted cuboctahedral shape. As shown in Fig. 1c, the cuboctahedral cage is also defined by the Co clusters as vertexes and organic linkers as edges. Two of the eight triangular faces of the cage are occupied by the tpt ligands, while the left ones and the quadrangular windows are open. The distance between the tpt defined faces is about 15 Å, excluding the van der Waals radius of atoms. Each cuboctahedral cage is connected with six identify cages by sharing the quadrangular faces (Fig. S2) and eight octahedral cages by sharing the triangular faces (Fig. 1d).

Interestingly, a novel nested cage structure (Fig. 1e) could be obtained when the interpenetration of individual networks is considered (Fig. 1f). Owing to the interpenetration, the smaller octahedral cages from one set of network is tightly nested in the larger cuboctahedral cages from the other set. The vertexes of octahedral cages locate at the center of the quadrangular windows of the cuboctahedral cages, and the triangular faces of these two kinds of cages arranged parallelly with different orientations. The tpt occupied faces in the nested cages stacked together with a 3.40 Å centroid-to-centroid distance between the triazine rings, indicating the presence of $\pi\text{--}\pi$ interaction between the rings. By considering the nested cages as the fundamental building unit, MOF

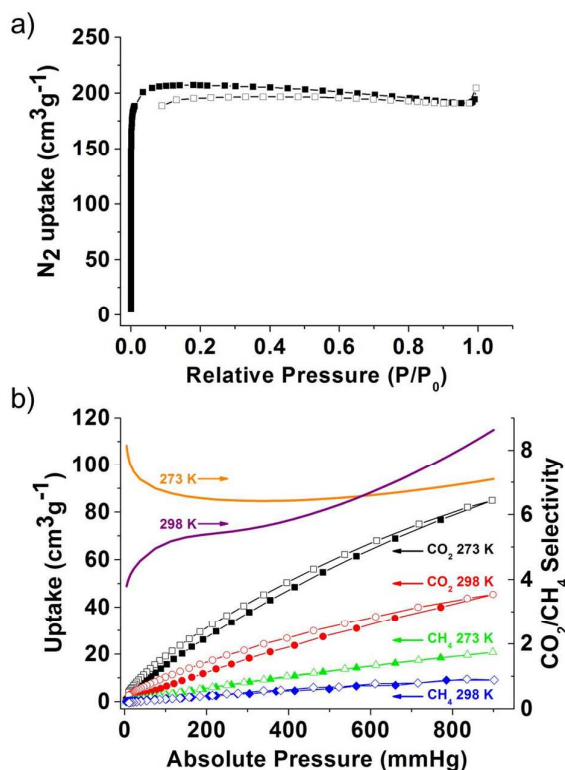


Fig. 2 Gas sorption properties of **1**: a) N_2 sorption isotherms at 77 K; (b) CO_2 and CH_4 sorption isotherms at 273 and 298 K (left Y axis) and the IAST-predicted selectivity for equimolar CO_2/CH_4 mixture as a function of total bulk pressure at 273 K and 298 K (right Y axis). The filled and open symbols represent for the adsorption and desorption data, respectively.

1 could be described as a “cage-in-cage” MOF based on interpenetrated networks. Though similar nested cage structure has been reported in polyhedron based MOFs constructed with planar triangular multi-tetrazole ligand as linkers,¹⁶ the realization of “cage-in-cage” MOFs through the combination of linear dicarboxylate ligand and planar triangular multi-pyridine ligand is quite rare, since the required matching of the configurations of the metal-contained nodes and the organic linkers is difficult to be predicted and designed. Then, MOF **1** provides a unique example of “cage-in-cage” MOFs.

The porous framework structure of **1** inspires us to investigate its gas sorption properties. The N_2 adsorption at 77 K was measured to evaluate the surface area (Fig. 2a). The type I isotherm indicates its microporous nature. The Brunauer-Emmett-Teller (BET) calculation gives a surface area of $637.5 \text{ m}^2 \text{ g}^{-1}$ for **1**. Furthermore, in order to investigate the CO_2 and CH_4 capture ability of MOF **1**, the corresponding adsorption isotherms were recorded at 273 and 298 K, respectively (Fig. 2b). For **1**, the maximum CO_2 adsorption at 900 mmHg are $84.89 \text{ cm}^3 \text{ g}^{-1}$ (273 K) and $45.38 \text{ cm}^3 \text{ g}^{-1}$ (298 K), respectively. The maximum CH_4 adsorption capacity of **1** at 900 mmHg are $20.74 \text{ cm}^3 \text{ g}^{-1}$ (273 K) and $9.08 \text{ cm}^3 \text{ g}^{-1}$ (298 K). In summary, though has moderate BET area, **1** exhibits comparable CO_2 and CH_4 adsorption with that of some other MOFs reported with similar or even larger surface area.¹⁷ To evaluate the interaction between the adsorbed guest molecules and the host framework, the CO_2 and CH_4 adsorption enthalpies (Q_{st}) of **1** were

calculated using the Virial method by fitting adsorption isotherms at 273 K and 298 K (for details, see ESI). The Q_{st} value of initial CO_2 adsorption is 28.9 kJ mol^{-1} (Fig. S7), while the corresponding Q_{st} value of CH_4 adsorption at zero loading is 14.4 kJ mol^{-1} . These Q_{st} values indicate relatively strong framework-guest interaction in **1** toward CO_2 , which is preferred for the selective CO_2 capture applications. Then, the CO_2/CH_4 adsorption selectivities of **1** at 273 and 298 K were calculated from the experimental single component isotherms using ideal adsorbed solution theory (IAST)¹⁸ to predict the CO_2 selective adsorption performance of **1** (for details, see ESI). As shown in Fig. 2b, the initial selectivity at 273 K reaches 8.1, and a decrease-increase trend was observed upon the increased pressure with a value of 7.0 reached at 900 mmHg. The selectivity at 298 K shows a continuous increase trend from 3.8 to 8.6. The selectivities at both temperatures are relatively lower than the reported MOFs with pre-designed CO_2 interaction motifs.¹⁹ From the structure point of view, the relatively high Q_{st} value and uptake of CO_2 should be attributed to the enhanced dipole-quadrupole interactions between the CO_2 molecules and the framework originated from the significant quadrupole moment of CO_2 ($-1.4 \times 10^{-39} \text{ cm}^2$), while the relatively low selectivity may indicate the competition of CO_2 and CH_4 for the identical sorption sites. Anyway, the increasing trend of selectivity at higher pressure with the raised temperature indicates the potential of the achievement of desirable selectivity at higher temperature and pressure.

In summary, a unique “cage-in-cage” MOF based on nested cages originated from the interpenetration has been constructed through the assembly of tpt and H_2bpdpc ligands with Co^{2+} ions. These results indicate that the interpenetration in MOFs could be utilized in modulating the structure of cage-based MOFs.

This work was supported by 973 Program of China (2014CB845600), the National Science Foundation of China (21290171, 21421001, and 21202088), and MOE Innovation Team of China (IRT13022).

Notes and references

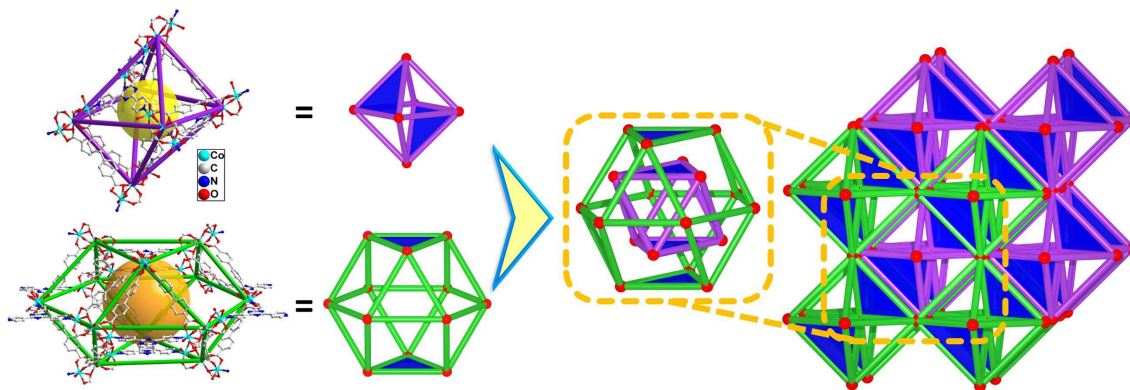
- ‡ Crystal data for **1** ($\text{C}_{60}\text{H}_{46}\text{Co}_3\text{N}_6\text{O}_{14}$): $M_r = 1251.82$, trigonal, space group $R\bar{3}c$, $a = b = 38.012(7)$, $c = 29.603(12)$ Å, $V = 37043(23)$ Å³, $Z = 18$, $\rho = 1.010 \text{ g cm}^{-3}$, $\mu = 0.647 \text{ mm}^{-1}$, $F(000) = 11538$, 89623 reflections measured, 7214 unique ($R_{\text{int}} = 0.126$), $R_1 = 0.0627$, $wR_2 = 0.1831$ [$I > 2\sigma(I)$]. CCDC reference number: 1046771
- 1 (a) H. C. Zhou, S. Kitagawa, *Chem. Soc. Rev.*, 2014, **43**, 5415; (b) L. J. Murray, M. Dincă and J. R. Long, *Chem. Soc. Rev.*, 2009, **38**, 1294; (c) C. Montoro, F. Linares, E. Q. Procopio, I. Senkovska, S. Kaskel, S. Galli, N. Masciocchi, E. Barea and J. A. Navarro, *J. Am. Chem. Soc.*, 2011, **133**, 11888; (d) S. Qiu, M. Xue and G. Zhu, *Chem. Soc. Rev.*, 2014, **43**, 6116; (e) Y. Cui, H. Xu, Y. Yue, Z. Guo, J. Yu, Z. Chen, J. Gao, Y. Yang, G. Qian and B. Chen, *J. Am. Chem. Soc.*, 2012, **134**, 3979; (f) Z. G. Guo, R. Cao, X. Wang, H. F. Li, W. B. Yuan, G. J. Wang, H. H. Wu and J. Li, *J. Am. Chem. Soc.*, 2009, **131**, 6894; (g) Q. Chen, Z. Chang, W.-C. Song, H. Song, H.-B. Song, T.-L. Hu and X.-H. Bu, *Angew. Chem., Int. Ed.*, 2013, **52**, 11550; (h) J. Yu, Y. Cui, C.-D. Wu, Y. Yang, B. Chen and G. Qian, *J. Am. Chem. Soc.*, 2015, **137**, 4026; (i) J. Liu, L. Chen and J. Zhang, L. Zhang and C.-Y. Su, *Chem. Soc. Rev.*, 2014, **43**, 6011; (j) Y. Han, N. F. Chilton, M. Li, C. Huang, H. Xu, H. Hou, B. Moubaraki, S. K. Langley, S. R. Batten, Y. Fan and K. S. Murray, *Chem. Eur. J.*, 2013, **19**, 6321; (k) H.-R. Fu, Z.-X. Xu and J. Zhang, *Chem. Mater.*, 2015, **27**, 205.
- 2 (a) B. Zheng, H. Dong, J. F. Bai, Y. Z. Li, S. H. Li and M. Scheer, *J. Am. Chem. Soc.*, 2008, **130**, 7778; (b) J. J. Perry Jr, J. A. Perman and M. J. Zaworotko, *Chem. Soc. Rev.*, 2009, **38**, 1400; (c) H. Wang, J. Xu, D.-S.

- Zhang, Q. Chen, R.-M. Wen, Z. Chang and X.-H. Bu, *Angew. Chem., Int. Ed.*, 2015, **54**, 5966; (d) X.-C. Huang, Y.-Y. Lin, J.-P. Zhang and X.-M. Chen, *Angew. Chem., Int. Ed.* 2006, **45**, 1557; (e) J.-R. Li and H.-C. Zhou, *Nat. Chem.* 2010, **2**, 893; (f) L. B. Sun, J. R. Li, W. Lu and H. C. Zhou, *J. Am. Chem. Soc.* 2012, **134**, 15923.
- 3 (a) A. Sonnauer, F. Hoffmann, M. Fröba, L. Kienle, V. Duppel, M. Thommes, C. Serre, G. Férey and N. Stock, *Angew. Chem., Int. Ed.*, 2009, **48**, 3791; (b) Y. Jiao, J. Zhang, L. Zhang, Z. Lin, C. He and C. Duan, *Chem. Commun.*, 2012, **48**, 6022.
 - 4 H. Deng, C. J. Doonan, H. Furukawa, R. B. Ferreira, J. Towne, C. B. Knobler, B. Wang and O. M. Yaghi, *Science*, 2010, **327**, 846.
 - 5 (a) Y.-L. Liu, V. C. Kravtsov, D. A. Beauchamp, J. F. Eubank and M. Eddaoudi, *J. Am. Chem. Soc.*, 2005, **127**, 7266; (b) J. H. Cavka, S. Jakobsen, U. Olsbye, N. Guillou, C. Lamberti, S. Bordiga and K. P. Lillerud, *J. Am. Chem. Soc.*, 2008, **130**, 13850; (c) F. J. Ma, S. X. Liu, C. Y. Sun, D. D. Liang, G. J. Ren, F. Wei, Y. G. Chen and Z. M. Su, *J. Am. Chem. Soc.*, 2011, **133**, 4178.
 - 6 (a) X. S. Wang, S. Q. Ma, P. M. Forster, D. Q. Yuan, J. Eckert, J. J. Lopez, B. J. Murphy, J. B. Parise and H. C. Zhou, *Angew. Chem., Int. Ed.*, 2008, **47**, 7263; (b) U. Stoeck, S. Krause, V. Bon, I. Senkovska and S. Kaske, *Chem. Commun.*, 2012, **48**, 10841.
 - 7 S.-T. Zheng, T. Wu, B. Irfanoglu, F. Zuo, P. Feng and X. Bu, *Angew. Chem., Int. Ed.*, 2011, **50**, 8034.
 - 8 D. Tian, Q. Chen, Y. Li, Y.-H. Zhang, Z. Chang and X.-H. Bu, *Angew. Chem., Int. Ed.*, 2014, **53**, 837.
 - 9 (a) H. L. Jiang, T. A. Makal and H. C. Zhou, *Coord. Chem. Rev.*, 2013, **257**, 2232; (b) Y.-Q. Chen, G.-R. Li, Z. Chang, Y.-K. Qu, Y.-H. Zhang and X.-H. Bu, *Chem. Sci.*, 2013, **4**, 3678.
 - 10 (a) G.-P. Yang, L. Hou, X.-J. Luan, B. Wu and Y.-Y. Wang, *Chem. Soc. Rev.*, 2012, **41**, 6992; (b) H. He, D. Yuan, H. Ma, D. Sun, G. Zhang and H. C. Zhou, *Inorg. Chem.*, 2010, **49**, 7605; (c) C. M. Nagaraja, B. Ugale and A. Chanthapally, *CrystEngComm*, 2014, **16**, 4805; (d) D. Singh and C. M. Nagaraja, *Cryst. Growth Des.*, 2015, DOI: 10.1021/acs.cgd.5b00450.
 - 11 W. G. Lu, C. Y. Su, T. B. Lu, L. Jiang and J. M. Chen, *J. Am. Chem. Soc.*, 2006, **128**, 34.
 - 12 X. Y. Dong, B. Li, B. B. Ma, S. J. Li, M.-M. Dong, Y. Y. Zhu, S. Q. Zang, Y. Song, H. W. Hou and T. C. Mak, *J. Am. Chem. Soc.*, 2013, **135**, 10214.
 - 13 A. L. Spek, *Acta Crystallogr., Sect. A*, 1990, **46**, C34, <http://www.cryst.chem.uu.nl/platon/platon>.
 - 14 (a) V. A. Blatov, A. P. Shevchenko and V. N. J. Serezhkin, *Appl. Crystallogr.*, 2000, **33**, 1193; (b) V. A. Blatov, L. Carlucci, G. Ciani and D. M. Proserpio, *CrystEngComm*, 2004, **6**, 378.
 - 15 Y.-Q. Chen, S.-J. Liu, Y.-W. Li, G.-R. Li, K.-H. He, Y.-K. Qu, T.-L. Hu and X.-H. Bu, *Cryst. Growth Des.*, 2012, **12**, 5426.
 - 16 M. Dincă, A. Dailly, C. Tsay and J. R. Long, *Inorg. Chem.*, 2008, **47**, 11.
 - 17 (a) E. E. Moushi, A. Kourtellaris, I. Spanopoulos, M. J. Manos, G. S. Papaefstathiou, P. N. Trikalitis and A. J. Tasiopoulos, *Cryst. Growth Des.* 2015, **15**, 185; (b) S. Pal, A. Bhunia, P. P. Jana, S. Dey, J. Möllmer, C. Janiak and H. P. Nayek, *Chem. Eur. J.* 2015, **21**, 2789; (c) R. Sen, D. Saha, S. Koner, P. Brandão and Z. Lin, *Chem. Eur. J.* 2015, **21**, 5962; (d) O. V. Gutov, W. Bury, D. A. Gomez-Gualdrón, V. Krungleviciute, D. Fairen-Jimenez, J. E. Mondloch, A. A. Sarjeant, S. S. Al-Juaied, R. Q. Snurr, J. T. Hupp, T. Yildirim and O. K. Farha, *Chem. Eur. J.* 2014, **20**, 12389; (e) S.-J. Bao, R. Krishna, Y.-B. He, J.-S. Qin, Z.-M. Su, S.-L. Li, W. Xie, D.-Y. Du, W.-W. He, S.-R. Zhang and Y.-Q. Lan, *J. Mater. Chem. A*, 2015, **3**, 7361.
 - 18 Y.-S. Bae, K. L. Mulfort, H. Frost, P. Ryan, S. Punnnathanam, L. J. Broadbelt, J. T. Hupp and R. Q. Snurr, *Langmuir*, 2008, **24**, 8592.
 - 19 (a) W.-Y. Gao, T. Pham, K. A. Forrest, B. Space, L. Wojtas, Y.-S. Chen and S. Ma, *Chem. Commun.*, 2015, **51**, 9636; (b) Y.-Q. Chen, Y.-K. Qu, G.-R. Li, Z.-Z. Zhuang, Z. Chang, T.-L. Hu, J. Xu and X.-H. Bu, *Inorg. Chem.*, 2014, **53**, 8842; (c) Z.-H. Xuan, D.-S. Zhang, Z. Chang, T.-L. Hu and X.-H. Bu, *Inorg. Chem.*, 2014, **53**, 8985.

Graphical Abstract

A Unique “Cage-in-Cage” Metal-Organic Framework based on Nested Cages from Interpenetrated Networks

Ting-Ting Zhou[†], Zhi-Hong Xuan[†], Da-Shuai Zhang, Ze Chang^{*}, Ying-Hui Zhang^{*}, and Xian-He Bu



A novel “cage-in-cage” metal organic framework was obtained based on nested cage structures originated from the two-fold interpenetrated networks composed of Co^{2+} ions, biphenyl-4,4'-dicarboxylic acid, and 2,4,6-tris(4-pyridyl)-1,3,5-triazine, which indicates the potential of interpenetration in structure modulation of cage-based MOFs.